Atomic scale investigation of a PbTiO3/SrRuO3/DyScO3 heterostructure

R. Egoavil, H. Tan, J. Verbeeck, S. Bals, B. Smith et al.

Additional information on Appl. Phys. Lett.
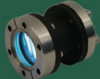
Atomic scale investigation of a PbTiO₃/SrRuO₃/DyScO₃ heterostructure

R. Egoavil,[1,a)] H. Tan,[1,2] J. Verbeeck,[1] S. Bals,[1] B. Smith,[3] B. Kuiper,[3] G. Rijnders,[3] G. Koster,[3] and G. Van Tendeloo[1]

[1]*EMAT, Department of Physics, University of Antwerp, Groenenborgerlaan 171, B-2020 Antwerp, Belgium*
[2]*CEMES-CNRS, Univ. de Toulouse, nMat Group BP94347, 31055, Toulouse Cedex 4, France*
[3]*Faculty of Science and Technology and MESA + Institute for Nanotechnology, University of Twente, P.O. Box 217, 7500 AE Enschede, The Netherlands*

An epitaxial PbTiO₃ thin film grown on self-organized crystalline SrRuO₃ nanowires deposited on a DyScO₃ substrate with ordered DyO and ScO₂ chemical terminations is investigated by transmission electron microscopy. In this PbTiO₃/SrRuO₃/DyScO₃ heterostructure, the SrRuO₃ nanowires are assumed to grow on only one type of substrate termination. Here, we report on the structure, morphology, and chemical composition analysis of this heterostructure. Electron energy loss spectroscopy reveals the exact termination sequence in this complex structure. The energy loss near-edge structure of the Ti–$L_{2,3}$, Sc–$L_{2,3}$, and O K edges shows intrinsic interfacial electronic reconstruction. Furthermore, PbTiO₃ domain walls are observed to start at the end of the nanowires resulting in atomic steps on the film surface. © *2013 AIP Publishing LLC*. [http://dx.doi.org/10.1063/1.4809597]

The study of ferroelectric thin films has become an important and exciting field of research within material science because of the many technological applications such as ferroelectric random access memories (FeRAMs),[1,2] nanocapacitors,[3] hybrid multiferroic nanostructures,[4] and ultrasonic sensors.[5] Intensive research has been focused on the study of the ferroelectric properties of Pb(ZrTi)O₃, BiFeO₃, (BaSr)TiO₃, and EuTiO₃ thin films deposited on different substrates.[2,6–8] An essential component to create a contact to these films is a metallic conductive SrRuO₃ oxide layer. Structural and physical properties as well as applications of SrRuO₃ have recently been extensively reviewed by Koster.[9] SrRuO₃ thin films have often been used as electrodes and their outstanding properties can be exploited in novel applications such as ferroelectric field-effect devices[10] and semiconductor spintronics.[11] SrRuO₃ may also serve as a model system for the atomistic growth of complex oxide materials.[9,12] Furthermore, nanostructuring on ferroelectric thin films in fabricating devices exhibit exceptional opportunities for future applications. Recently, epitaxially grown SrRuO₃ thin films were used as an intermediate layer between a ferroelectric PbTiO₃ film and a DyScO₃ substrate, to shape the ferroelectric domains walls in the PbTiO₃.[7] Moreover ultra-thin SrRuO₃ films grown on SrTiO₃ are found to be insulating instead of a metallic and ferromagnetic below 4 monolayers. A possible interfacial antiferromagnetic layer is suggested[13] but not observed directly. Here, we provide a thorough structural and chemical characterization at the atomic scale, leading to a major understanding of the growth of SrRuO₃ as well as the subsequent PbTiO₃ thin film.

Particularly interesting is the self-organized formation of epitaxial SrRuO₃ ribbon-like structures on SrTiO₃ and LaAlO₃ substrate steps. SrRuO₃ nanostructures are reported to nucleate on substrate steps followed by a 3D island growth.[14,15] Recent work reported that SrRuO₃ nanowires grow preferentially only on one type of DyScO₃ surface termination. A diffusion model was proposed where a difference in surface diffusion between DyO and ScO₂ was responsible for the formation of the SrRuO₃ nanowires.[12] Although many investigations concerning these complex heterostructures have been reported, most of the information is supported by atomic force microscopy (AFM) and/or scanning tunneling microscopy (STM), and, there is no direct information on the interface termination sequence. Here, we provide direct evidence for the growth of the nanowires on ScO₂ terminated regions.

In addition, the aim of the present paper is to directly determine the exact stacking of the atomic planes at the SrRuO₃/DyScO₃ as well as PbTiO₃/DyScO₃ interfaces. A detailed atomic model of the interfaces is proposed which is confirmed by the excellent match between experimental and simulated images based on the proposed structure. Finally, the atomic structure of the PbTiO₃ film has been investigated.

A nanostructured multilayer sample was grown by pulsed laser deposition (PLD). An epitaxial thin film of PbTiO₃ with ∼30 nm thickness was deposited on a configuration of self-assembled ∼5 nm high SrRuO₃ nanowires deposited on a mixed termination (110)DyScO₃ substrate. More details of the sample growth conditions can be found in Refs. 12 and 16. The lattice parameters of PbTiO₃ are $a = b = 3.894$ Å and $c = 4.14$ Å. The orthorhombic SrRuO₃ and DyScO₃ can be considered as pseudo-cubic structures with $a = 3.93(4)$ Å.[6,7] To investigate the sample using transmission electron microscopy, a lamella was prepared perpendicular to the [001] zone axis orientation of the DyScO₃ substrate using focused ion beam milling. The atomic resolution high angle annular dark field (HAADF), scanning transmission electron microscopy (STEM), and electron energy loss spectroscopy (EELS) experiments were performed using a FEI Titan[3] microscope operated at 120 kV, equipped with an aberration corrector for both image and probe forming lenses, and a monochromator to optimize the energy resolution for EELS measurements up to 300 meV, as determined from the full width at half maximum (FWHM) of the zero

a)ricardo.egoavil@ua.ac.be

loss peak. The STEM convergence semi-angle α used was $\sim$18 mrad, providing a spatial resolution of $\sim$1.4 Å (probe size). The collection semi-angle β of the spectrometer was estimated to be $\sim$173 mrad. For HAADF-STEM imaging, an inner detector semi-angle of $\sim$70.4 mrad was used. The quantitative elemental maps and profiles were generated by subtracting a power law background and integrating the corresponding core-loss excitation edge for each chemical element. Sample thickness variation effects are minimized by normalizing each element signal with respect to the O signal averaged over a unit cell, which is assumed to be constant. The HAADF-STEM image simulations were performed using the STEMSIM software package (see supplementary material[26]).

Figure 1(a) shows a HAADF-STEM overview of the sample at low magnification. A sequence of discrete $SrRuO_3$ nanowires on the substrate was visible as $\sim$5 nm high and $\sim$120 nm wide (dark regions). These $SrRuO_3$ structures are approximately 20–25 nm apart from each other.

Two-dimensional spectrum images were acquired with STEM-EELS to investigate the spatial distribution of the elements within the sample (white box in Figure 1(a)). Quantitative elemental maps corresponding to Ru-$M_{4,5}$, Sc-$L_{2,3}$, Ti-$L_{2,3}$, and O-K edges were generated. The corresponding color map with Sc (red), Ti (blue), and Ru (light-blue) of this
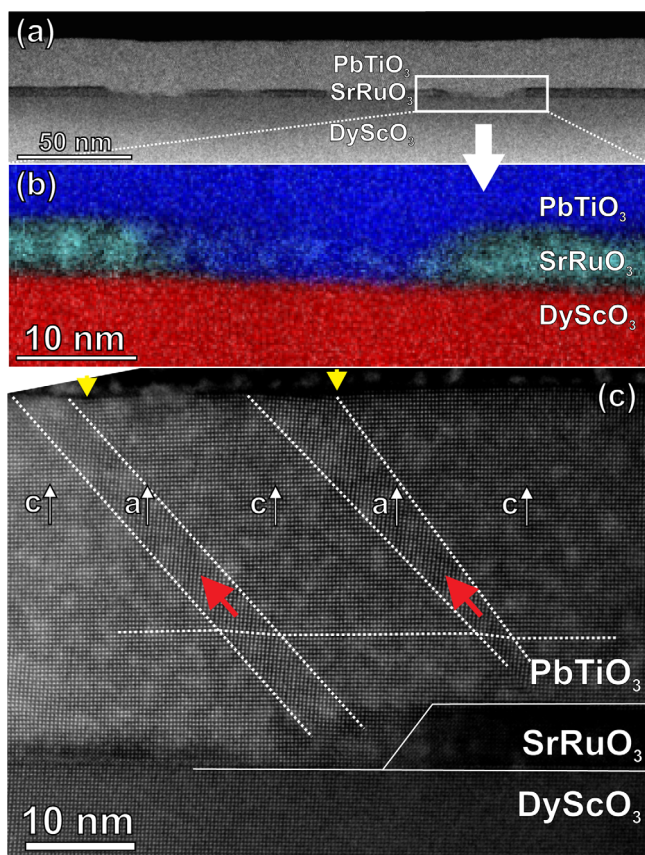
region is shown in Figure 1(b). The distinct sample areas can clearly be identified as $PbTiO_3$ (blue), $SrRuO_3$ (light-blue), and $DyScO_3$ (red).

Domain walls are visible in the $PbTiO_3$ film (white dashed-lines) predominantly starting from the end of the nanowires (Figure 1(c)). These walls are observed to reach the surface of the film resulting in nanometer surface steps of $\sim$1–2 nm high (yellow arrows). The two a and c domains characteristic of the $PbTiO_3$ film are indicated by the white vertical arrows. This observation provides direct evidence that the domain periodicity is patterned by the nanowires and shows excellent agreement with AFM and piezoresponse force microscopy (PFM) measurements (not shown). Such measurements show that some ac-domains do line up along the edges of the wires, whereas the remaining ac-domains are distributed periodically along the wires.[16]

Figure 2(a) shows a high resolution HAADF-STEM image of the sample. The a and c directions of the $PbTiO_3$ film are indicated by arrows. The pseudo-cubic arrangement of the (110)-surface $DyScO_3$ facilitates the coherent growth of $PbTiO_3$ and $SrRuO_3$ thin films.[17,18] Next, we will investigate the interface arrangement between the different layers. A wide dark band of $\sim$1.19 nm at the $PbTiO_3/SrRuO_3$ interface and a sharp dark line of $\sim$0.37 nm at $SrRuO_3/DyScO_3$ interface are observed and marked by the white arrows. HAADF intensity line profiles in Figure 2(b) were measured across the interfaces in regions containing a nanowire or without a nanowire (Figure 2(a)). All line intensity profiles were integrated over a width of 0.1 nm. Across a $SrRuO_3$ nanowire, two interfaces are encountered and the line profile
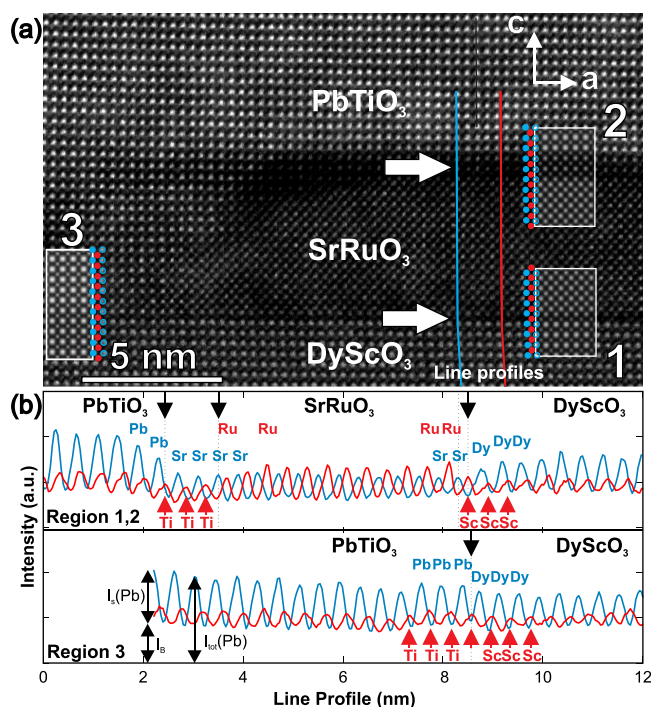

FIG. 1. (a) HAADF-STEM overview image of the sample. The surface structure of the $PbTiO_3$ film and the $SrRuO_3$ nanowires of $\sim$5 × 120 nm size is distinct. (b) Colored elemental map with Ti (blue), Ru (light-blue), and Sc (red). (c) Magnified image of a nanowire ending showing the a and c domains in the $PbTiO_3$ film. Domain walls in the film (white dashed-lines) occur (mostly) at the end of the nanowires. The horizontal dashed-line indicates the bending of an atomic plane through ac-domains.

FIG. 2. (a) High resolution HAADF-STEM image taken shows two dark bands in both $PbTiO_3/SrRuO_3$ and $SrRuO_3/DyScO_3$ interfaces indicated by arrows. (b) Line profiles across a $SrRuO_3$ nanowire indicate the atomic sequence in both interfaces (regions 1 and 2) with alternating Pb-Sr-Dy (blue) and Ti-Ru-Sc (red). Line profiles in a region without nanowire (regions 3) show alternating Pb-Dy (blue) and Ti-Sc (red). The insets 1, 2, and 3 in (a) indicate the simulated images.

can either cross the Pb, Sr, and Dy (blue line) atoms or half a unit cell shifted it crosses the Ti, Ru, and Sc (red line) atoms. In a region without nanowire, the lines can either cross Pb and Dy atoms or half a unit cell further the Ti and Sc atoms. The image intensities of these line profiles are plotted in Figure 2(b). From this plot, we note differences in intensities of the different atom as is to be expected since the HAADF STEM intensity scales with the average atomic weight of a column (known as Z-contrast). Unfortunately, the average atomic weights of the different columns are not much different: Ti ($Z = 22$) and Sc ($Z = 21$), hampering an unambiguous determination of the stacking sequence. This problem can be overcome by using STEM EELS.

Using STEM EELS, 2D spectrum images were acquired for regions with and without $SrRuO_3$ nanowires. Atomically resolved elemental maps are shown in Figures 3(a) and 3(b). From these maps, we observe that the $DyScO_3$ substrate is Sc-terminated (red columns in Figure 3(a)) under a nanowire and Dy-terminated (green columns in Figure 3(b)) in case the nanowire is absent. Figure 3(c) shows the elemental profiles for Dy, Sc, Ti, Sr, and Ru obtained across the interfaces. For clarity, all profiles are shifted along the vertical axis and the corresponding interfaces are indicated by black arrows (regions 1, 2, and 3 in Figure 2(a)). At the $SrRuO_3/DyScO_3$ interface, the $DyScO_3$ is ScO_2 terminated and $SrRuO_3$ is SrO terminated (region 1). It is clear that a large region at the interface between $PbTiO_3$ and $SrRuO_3$ contains Ti, Sr, and oxygen (region 2). This region coincides with the darker region in the HAADF image. It can be estimated that a region of 3 unit cells of $SrTiO_3$ has formed at this interface. The fact that the Ti signal does not reach zero in the $SrRuO_3$ nanowire is likely an artefact of the quantification caused by the proximity of the Sc-$L_{2,3}$ edge (402 eV) to the Ti-$L_{2,3}$
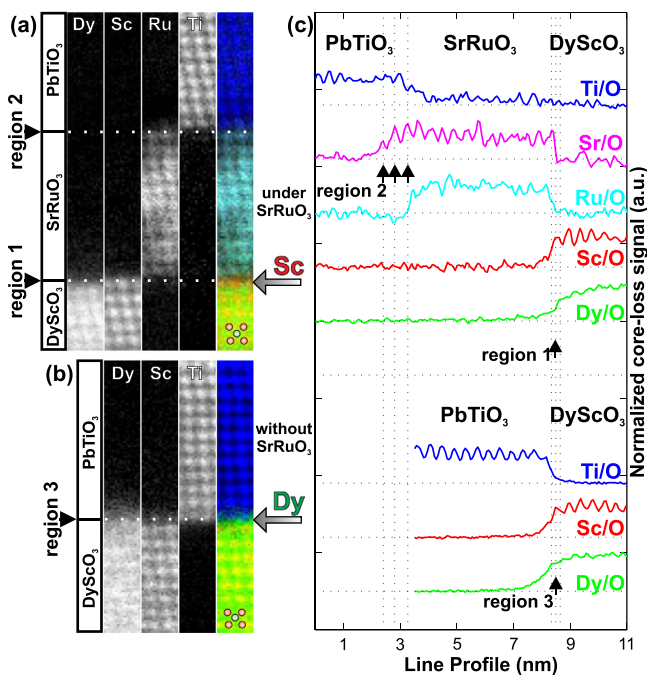
edge (456 eV), hampering precise background subtraction. At the $PbTiO_3/DyScO_3$ interface, $DyScO_3$ is DyO terminated whereas $PbTiO_3$ is TiO_2 terminated (region 3). This is in agreement with the HAADF contrast present in simulations assuming this structure (insets 1, 2, and 3 in Figure 2). No clear interdiffusion is observed and all profiles have a similar steepness at the interfaces.

Also the electronic structure at the interfaces is investigated. Figure 4 shows EELS spectra of Ti-$L_{2,3}$, Sc-$L_{2,3}$, and O-K edges. The core loss spectral shapes are presented for positions 1-9 across the interfaces of a $SrRuO_3$ nanowire.

At the $SrRuO_3/DyScO_3$ interface, the e_g/t_{2g} ratio of the Sc-$L_{2,3}$ edge is decreased at the interface (spectrum 4). The t_{2g} state of the L_3 edge (red arrow) at this interface is higher in energy, which indicates an electronic-structure reconstruction as a result of the subsequent growth of $SrRuO_3$. In contrast, a gradual change in the Ti-$L_{2,3}$ and O-K edges is clearly seen, going from the $PbTiO_3/SrRuO_3$ interface (spectra 5–6) into the ones acquired further in the $PbTiO_3$ film (spectra 7–9). These changes can be attributed to changes in electronic structure. Electronic-structure changes at this interface result in higher energy e_g and t_{2g} states (black arrows), and an increased e_g/t_{2g} ratio (as compared to the $PbTiO_3$ film – red arrows), attributed to a region of $SrTiO_3$ with Ti^{+4} which has formed at this interface. The results show good agreement with the results obtained by Eberg[19] concerning an epitaxial $PbTiO_3$ thin film grown on a $SrTiO_3$ substrate. Moreover, the four clear peaks in the Ti-$L_{2,3}$ edge characteristic for Ti^{+4} become broader at the interface (spectrum 5), with a reduced peak separation. This broadening is attributed to the Ti^{+3} component as reported in Refs. 20–25.

The combination of HAADF-STEM and EELS enables us to suggest a detailed atomic model of the growth mechanism. The exact termination sequence of the interfaces was determined and the corresponding simulated images are
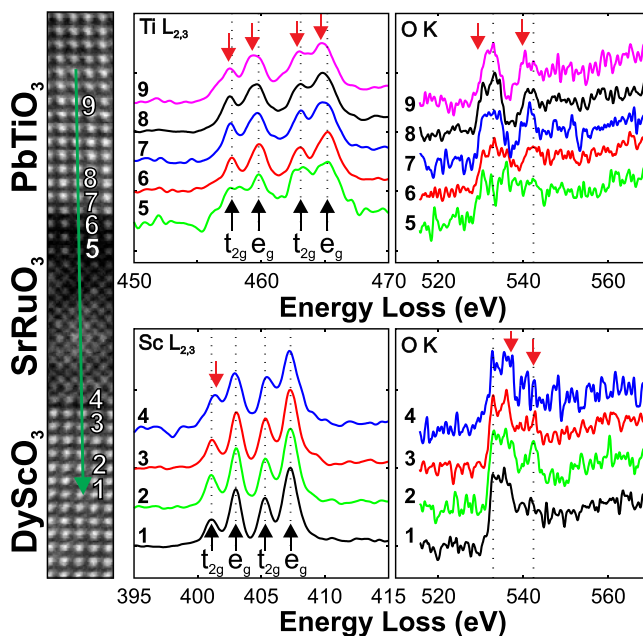

FIG. 3. ((a), (b)-left) Elemental maps of Dy-$L_{2,3}$, Sc-$L_{2,3}$, Ru-$M_{4,5}$, and Ti-$L_{2,3}$ edges (gray scaled) together with the corresponding color map with Dy (green), Sc (red), Ru (light-blue), and Ti (blue) from (a) region 1, 2 and (b) region 3. (c) Atomic elemental line profiles with Dy (green), Sc (red), Ru (light-blue), Sr (pink), and Ti (blue) crossing the interfaces.

FIG. 4. EELS spectra of Ti-$L_{2,3}$, Sc-$L_{2,3}$, and O K edges across the $SrRuO_3$ nanowire. Subtle changes are observed as a result of an electronic-structure reconstruction at the $PbTiO_3/SrRuO_3$ and $SrRuO_3/DyScO_3$ interfaces.
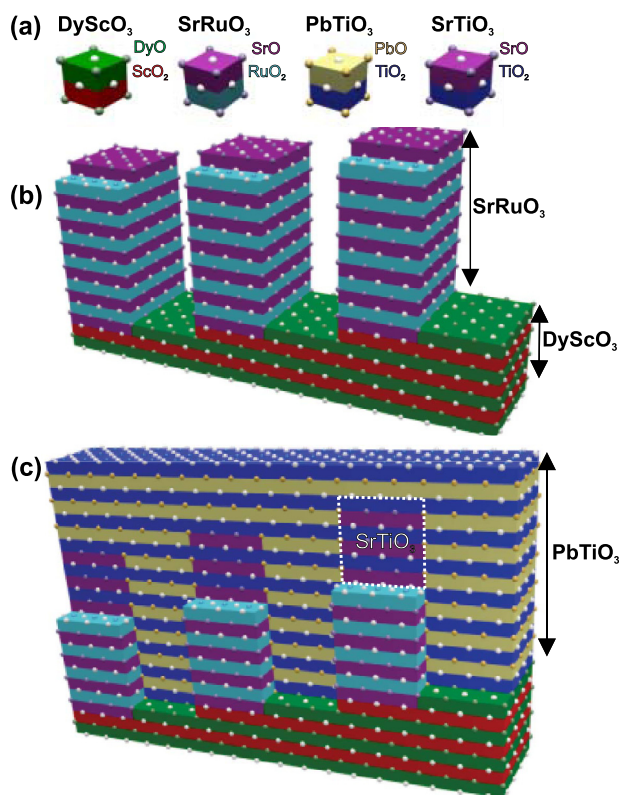
FIG. 5. 3D model of the growth system: (a) Perovskite building blocks of DyScO₃, SrRuO₃, PbTiO₃, and SrTiO₃. AO and BO₂ layers are shown in a distinct color. (b) SrRuO₃ grows preferentially on Sc-terminated DyScO₃ substrate steps. (c) Epitaxial growth of the PbTiO₃ film inducing an unexpected 3 unit cells of SrTiO₃.

shown in Figure 2 (insets 1, 2, and 3). Figure 5 shows a three dimensional (3D) representation of the proposed model. The perovskite fundamental ABO_3 building blocks of DyScO₃, SrRuO₃, PbTiO₃, and SrTiO₃ are depicted in Figure 5(a), with differently colored AO and BO_2 layers. The mixed terminated DyScO₃ substrate is shown, with SrRuO₃ nanowires aligning along the ScO_2 terminated layers. Subsequent growth of SrRuO₃ results in a nanowire pattern (Figure 5(b)). Our results show that further epitaxial growth of the PbTiO₃ thin film results in an unexpected 3 unit cells of SrTiO₃ (Figure 5(c)).

The presence of the SrTiO₃ layer is most likely to be related to the high volatility of Ru, which can be evaporated from the surface during the deposition as is stated by Koster.[9] This argument is strongly supported by the results obtained from a similar complex structure by using a continuous atomically flat interlayer of ∼5 nm SrRuO₃ between the PbTiO₃ film and the DyScO₃ substrate. Results show substantial Ru deficiency at both PbTiO₃/SrRuO₃ and SrRuO₃/DyScO₃ interfaces (see supplementary material[26]). In addition, the presence of Ru in between the SrRuO₃ wires as shown in Figure 1(b) suggests that part of the Ru also diffuses into the PbTiO₃ layer in between the nanowires leading an SrTiO₃ layer at the top of SrRuO₃.

In the context of this work, the most important conclusion from atomically resolved EELS characterization is that the preferential growth of the SrRuO₃ occurs on the terraces of the Sc-terminated DyScO₃ substrate instead of Dy-terminated.

Atomically resolved EELS plays a key role to determine the exact atomic stacking sequence. The formation of an insulating SrTiO₃ layer has important implications, especially when using SrRuO₃ as a bottom electrode. Understanding and control of the growth mechanisms are crucial since they determine the physical properties of the films. The structural domains walls surface-patterned in the film are strongly related to the location of the SrRuO₃ nanowires. These observations will serve as feedback to the growth process and will help to understand ferroelectric properties of these films.

[1] J. F. Scott and C. A. Araujo, Science **246**, 1400–1405 (1989).
[2] J. F. Scott and C. A. Araujo, Science **315**, 954–959 (2007).
[3] M. M. Saad, P. Baxter, R. M. Bowman, J. M. Gregg, F. D. Morrison, and J. F. Scott, J. Phys.: Condens. Matter **16**, L451–L456 (2004).
[4] T. N. Narayanan, B. P. Mandal, A. K. Tyagi, A. Kumarasiri, X. Zhan, M. G. Hahm, M. R. Anantharaman, G. Lawes, and P. M. Ajayan, Nano Lett. **12**, 3025–3030 (2012).
[5] K. Yamashita, H. Murakami, M. Okuyama, T. Tanaka, Y. Mo, A. Tsuchitani, and Y. Suzuki, J. Korean Phys. Soc. **42**, S1108–S1112 (2003).
[6] S. J. Callori, J. Gabel, D. Su, J. Sinsheimer, M. V. Fernandez-Serra, and M. Dawber, Phys. Rev. Lett. **109**, 067601 (2012).
[7] S. Venkatesan, B. J. Kooi, and J. T. M. De Hosson, J. Appl. Phys. **102**, 104105 (2007).
[8] D. G. Schlom, L.-Q. Chen, C.-B. Eom, K. M. Rabe, S. K. Streiffer, and J.-M. Triscone, Annu. Rev. Mater. Res. **37**, 589–626 (2007).
[9] G. Koster, L. Klein, W. Siemons, G. Rijnders, J. S. Dodge, C.-B. Eom, D. H. A. Blank, and M. R. Beasley, Rev. Mod. Phys. **84**(1), 253–298 (2012).
[10] C. H. Ahn, R. H. Hammond, T. H. Geballe, M. R. Beasley, J.-M. Triscone, M. Decroux, Ø. Fischer, L. Antognazza, and K. Char, Appl. Phys. Lett. **70**, 206 (1997).
[11] D. D. Awschalom and M. E. Flatté, Nat. Phys. **3**, 153–159 (2007).
[12] B. Kuiper, J. L. Blok, H. J. W. Zandvliet, D. H. A. Blank, G. Rijnders, and G. Koster, MRS Commun. **1**, 17–21 (2011).
[13] J. Xia, W. Siemons, G. Koster, M. R. Beasley, and A. Kapitulnik, Phys. Rev. B **79**, 140407(R) (2009).
[14] E. Vasco, R. Dittmann, S. Karthäuser, and R. Waser, Appl. Phys. Lett. **82**(15), 2497–2499 (2003).
[15] F. Sánchez, G. Herranz, I. C. Infante, C. Ferrater, M. V. Garcia-Cuenca, M. Varela, and J. Fontcuberta, Prog. Solid State Chem. **34**, 213–221 (2006).
[16] B. Smith, B. Kuiper, A. ten Elshof, G. Rijnders, S. Bals, J. Verbeeck, G. Van Tendeloo, and G. Koster, "Domain engineering in ferroelectric thin films through nano-patterned bottom electrodes" (unpublished).
[17] J. E. Kleibeuker, G. Koster, W. Siemons, D. Dubbink, B. Kuiper, J. L. Blok, C.-H. Yang, J. Ravichandran, R. Ramesh, J. E. ten Elshof *et al.*, Adv. Funct. Mater. **20**, 3490–3496 (2010).
[18] G. Catalan, A. Janssens, G. Rispens, S. Csiszar, O. Seeck, G. Rijnders, D. H. A. Blank, and B. Noheda, Phys. Rev. Lett. **96**, 127602 (2006).
[19] E. Eberg, A. T. J. van Helvoort, R. Takahashi, M. Gass, B. Mendis, A. Bleloch, R. Holmestad, and T. Tybell, J. Appl. Phys. **109**, 034104 (2011).
[20] H. W. Jang, D. A. Felker, C. W. Bark, Y. Wang, M. K. Niranjan, C. T. Nelson, Y. Zhang, D. Su, C. M. Folkman, S. H. Baek *et al.*, Science **331**, 886 (2011).

[21]M. Watanabe, E. Okunishi, and K. Ishizuka, Microscopy and Analysis **23**, 5–7 (2009).

[22]M. R. Keenan and P. G. Kotula, Surf. Interface Anal. **36**, 203–212 (2004).

[23]A. Rosenauer and M. Schowalter, *Springer Proceedings in Physics: Microscopy of Semiconducting Materials* (Springer, New York, 2007), Vol. 120, p. 169.

[24]J. Verbeeck, P. Schattschneider, and A. Rosenauer, Ultramicroscopy **109**, 350–360 (2009).

[25]J. Verbeeck, A. Béché, and W. Van den Broek, Ultramicroscopy **120**, 35–40 (2012).

[26]See supplementary material at http://dx.doi.org/10.1063/1.4809597 for details about the HAADF-STEM image simulation parameters and the analysis of a continuous interlayer of $SrRuO_3$.